ARTICLE

Control of SOX2 protein stability and tumorigenic activity by E3 ligase CHIP in esophageal cancer cells

Li Kang[1,8], Huifang Zhang[1,8], Yaling Wang[1,8], Manyu Chu[2], Jianzhong He[2], Mengyang Xue[3,4], Liu Pan[4,5], Yunfeng Zhang[1], Zhen Wang[6], Zhaosu Chen[1], Yuanyong Huang[1], Zitai Chen[1], Enmin Li[7], Jiwen Li[1], Liyan Xu[2], Rong Zhang[4]✉ and Jiemin Wong[1]✉

SOX2 is highly expressed and controls tumor initiation and cancer stem cell function in various squamous cell carcinomas including esophageal squamous cancer. However, the molecular mechanism leading to SOX2 overexpression in cancer is incompletely understood. Here, we identified CHIP, a chaperone-associated ubiquitin E3 ligase, as a novel negative regulator of SOX2 protein stability and tumorigenic activity in esophageal squamous carcinoma cells. We showed that CHIP interacted with SOX2 primarily via chaperone HSP70, together they catalyzed SOX2 ubiquitination and degradation via proteasome. In contrast, HSP90 promoted SOX2 stability and inhibition of HSP90 activity induced SOX2 ubiquitination and degradation. Notably, unlike the case in normal esophageal tissues where CHIP was detected in both the cytoplasm and nucleus, CHIP in clinical esophageal tumor specimens was predominantly localized in the cytoplasm. Consistent with this observation, we observed increased expression of exportin-1/CRM-1 in clinical esophageal tumor specimens. We further demonstrated that CHIP catalyzed SOX2 ubiquitination and degradation primarily in the nuclear compartment. Taken together, our study has identified CHIP as a key suppressor of SOX2 protein stability and tumorigenic activity and revealed CHIP nuclear exclusion as a potential mechanism for aberrant SOX2 overexpression in esophageal cancer. Our study also suggests HSP90 inhibitors as potential therapeutic agents for SOX2-positive cancers.

Oncogene (2023) 42:2315–2328; https://doi.org/10.1038/s41388-023-02745-z

Graphical Abstract

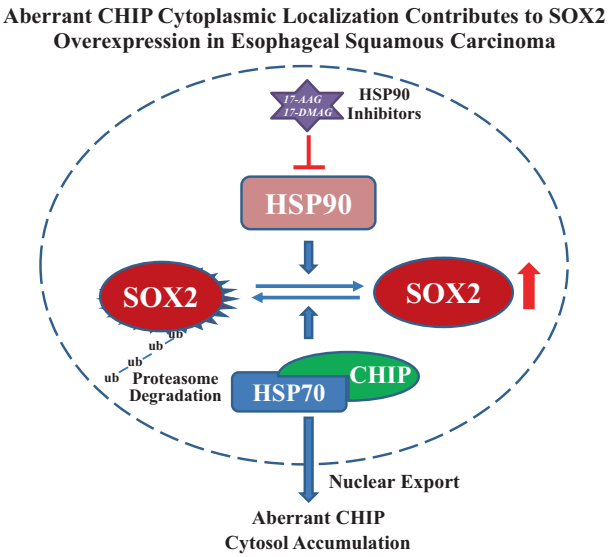

[1]Shanghai Key Laboratory of Regulatory Biology, Fengxian District Central Hospital-ECNU Joint Center of Translational Medicine, Institute of Biomedical Sciences and School of Life Sciences, East China Normal University, Shanghai 200241, China. [2]Guangdong Provincial Key Laboratory of Infectious Diseases and Molecular Immunopathology, Institute of Basic Medical Science, Cancer Research Center, Shantou University Medical College, Shantou, Guangdong, China. [3]The Third School of Clinical Medicine, Southern Medical University, Guangzhou, China. [4]Department of Obstetrics and Gynecology, ECNU Joint Center of Translational Medicine, Fengxian Central Hospital affiliated to the Southern Medical University, Shanghai, China. [5]Department of Obstetrics and Gynecology, Jinzhou Medical University, Liaoning, China. [6]Department of Endocrinology, Shandong Provincial Hospital Affiliated to Shandong First Medical University, Jinan, Shandong, China. [7]Key Laboratory of Molecular Biology for High Cancer Incidence Coastal Chaoshan Area, Department of Biochemistry and Molecular Biology, Shantou University Medical College, Shantou, Guangdong, China. [8]These authors contributed equally: Li Kang, Huifang Zhang, Yaling Wang. ✉email: rongzhang@163.com; jmweng@bio.ecnu.edu.cn

Received: 7 December 2022 Revised: 5 May 2023 Accepted: 5 June 2023
Published online: 23 June 2023

INTRODUCTION

Transcription factor SOX2, a member of the large family of SRY-related HMG box transcription factors, is well known for its critical role in maintaining embryonic and tissue stem cells and establishing induced pluripotent stem cells [1–4]. However, mounting evidence has linked aberrant SOX2 overexpression to human malignancies [5–11]. For instance, SOX2 was identified as the most upregulated transcription factor in the skin squamous cell carcinoma and had critical roles in tumor initiation and cancer stem cell function [12]. Transgenic SOX2 overexpression combined with Cdkn2ab and Pten loss is sufficient to drive lung squamous cell carcinoma from different cells of origin [5]. Furthermore, elevated SOX2 has been shown to promote lineage plasticity and antiandrogen resistance in TP53- and RB1-deficient prostate cancer [6]. Collectively, accumulative studies indicate that elevated SOX2 expression promotes cell proliferation, invasion, migration, and metastasis, evades apoptotic signals, and controls tumor initiation and cancer stem cell functions in squamous cell carcinoma and other cancers [7, 8, 10, 13, 14]. Thus, a central task regarding SOX2 is to understand the molecular mechanisms leading to aberrant SOX2 overexpression in cancers.

Esophageal cancer is the sixth leading cause of cancer-related deaths worldwide [15–17]. Accumulating evidence underscores SOX2 overexpression as a key driving factor for esophageal squamous cell carcinoma (ESCC), the predominant form (~85%) of esophageal cancer that lacks targeted therapeutics [16, 18–21]. As a mechanism for aberrant SOX2 expression in cancers, SOX2 gene amplification was first detected as a recurrent event in ESCC and lung cancers, in which SOX2 functioned as a lineage-survival oncogene [18, 22, 23]. Since then, SOX2 gene amplification has been reported in multiple types of squamous cancers and glioblastoma [21, 24]. However, gene amplification alone could not account for widespread aberrant SOX2 overexpression in cancers [25]. As a transcription factor with potent activity in transcription and cell fate determination, we and others have demonstrated that SOX2 is tightly regulated at the level of protein stability and is subjected to rapid turnover by various ubiquitin E3 ligase-mediated proteasome degradation [12, 24, 26–29]. In this regard, several kinases have been shown to drive SOX2 overexpression in cancers by promoting SOX2 protein stability. For example, AKT, a kinase most frequently hyperactivated in cancers, phosphorylates SOX2 and protects SOX2 from ubiquitination by E3 ligases WWP2 and UBR5 and degradation by proteasome in ESCC and glioblastoma [26, 27, 29]. DNA-dependent protein kinase (DNA-PK) has also been reported to sustain glioma stem cells by promoting SOX2 stability via preventing WWP2-mediated ubiquitination [30]. Thus, identification of molecular mechanisms driving aberrant SOX2 overexpression in cancers is not only essential for better understanding of SOX2 oncogenic function, but also for devising novel therapeutic approaches for various cancers driven by aberrant SOX2 overexpression.

In this study, we identified CHIP (carboxyl terminus of Hsc70-interaction protein) as a ubiquitin E3 ligase that targets SOX2 for ubiquitin-dependent proteasome degradation in ESCC cells. As a ubiquitin E3 ligase interacting with HSP70 and HSP90 molecular chaperones, CHIP has a critical role in maintaining cellular and organismal protein homeostasis [31–33]. We present evidence that CHIP interacts with and targets SOX2 for ubiquitination and proteasome-dependent degradation via HSP70. In the contrary to HSP70, HSP90 promotes SOX2 stability and inhibition of HSP90 activity instigates SOX2 degradation in a CHIP-dependent manner. Notably, we observed in clinical esophageal squamous tumors that CHIP is predominantly distributed in the cytoplasm, and further study revealed that CHIP targets SOX2 degradation mainly in the nuclear compartment. Our study revealed aberrant CHIP subcellular localization as a potential mechanism driving SOX2 overexpression in ESCC tumors and identified HSP90 inhibitors as possible therapeutic agents for SOX2 positive ESCC cancer.

RESULTS

CHIP negatively controls SOX2 protein stability through proteasome degradation

Given its role in protein quality control and beyond [31–33], we investigated if CHIP regulates SOX2 protein stability and function in esophageal cancer cells. We knocked down CHIP as well as several other E3 ligases that have been implicated in SOX2 degradation or interaction in two esophageal cancer cell lines, K30 and K450 [26, 27, 29, 34], by lentiviral transduction of corresponding specific short hairpin RNA (shRNA). Consistent with previous studies [29, 30], knockdown of either UBR5 or WWP2 led to elevated levels of SOX2, indicating these two E3 ligases play roles in promoting SOX2 turnover (Fig. 1A). Notably, knockdown of CHIP also substantially increased the level of SOX2 protein (Fig. 1A), suggesting a role of CHIP in control of SOX2 proteostasis. To substantiate this finding, we knocked down CHIP in K30 and K450 cells by two distinct CHIP-specific shRNAs and confirmed that knockdown of CHIP indeed resulted in elevated levels of SOX2 protein (Fig. 1B). Knockdown of CHIP had no significant effect on the levels of SOX2 mRNA in both K30 and K450 cells, as revealed by quantitative reverse transcription PCR (RT-qPCR) (Fig. 1C). We then ectopically overexpressed a FLAG tagged CHIP in both cell lines and observed that overexpression of FLAG-CHIP markedly down-regulated the levels of SOX2 protein (Fig. 1D) but did not significantly affect the levels of SOX2 mRNA (Fig. 1E). Together these results suggested a role of CHIP in downregulation of SOX2 protein post-transcriptionally.

To test whether CHIP downregulates SOX2 through proteasome degradation, we ectopically overexpressed FLAG-CHIP and treated the transfected cells with or without MG132, a proteasome inhibitor. The representative results in Fig. 1F showed that CHIP overexpression-induced downregulation of SOX2 was blocked by treatment with 10 μg/ml MG132 for 8 h, indicating that CHIP most likely downregulates SOX2 through proteasome-dependent degradation. In agreement with this idea, cycloheximide chase assay revealed that knockdown of CHIP significantly extended, whereas ectopic overexpression of CHIP markedly shortened the half-life of SOX2 proteins (Fig. 1G, H).

We also examined how knockdown of CHIP affected SOX2 protein level by immunofluorescent staining assay. The representative results in Fig. 1I showed that knockdown of CHIP with two distinct shRNAs resulted in marked elevation of SOX2 protein in both K30 and K450 cells. In contrast, ectopic overexpression of CHIP downregulated the level of SOX2 protein and this down-regulation of SOX2 could be blocked by addition of MG132 (Fig. 1J).

Altogether these results unraveled a role of CHIP in controlling SOX2 protein stability by targeting SOX2 for proteasome-dependent degradation.

CHIP Downregulates SOX2 in a HSP70 and E3 Ligase Activity-Dependent Manner

As a chaperone-mediated E3 ligase, CHIP has been shown to selectively target p53 [35], AKT [36], c-MYC [37], and UHRF1 [38] for degradation. Having observed that CHIP instigated SOX2 degradation, we compared the effect of CHIP on SOX2 with these reported substrate proteins. As shown in Fig. 2A, ectopic overexpression of CHIP downregulated SOX2 in both K30 and K450 cells more potently than p53, AKT1 and c-MYC. Similarly, knockdown of CHIP upregulated SOX2 level more significantly than p53, AKT1 and c-MYC (Fig. 2B), thus rendering SOX2 as a bona fide CHIP substrate.

Given CHIP as a chaperone-associated ubiquitin E3 ligase, we next investigated the role of chaperones HSP70 and HSP90 in CHIP-mediated SOX2 degradation. First, co-immunoprecipitation (IP) assay revealed that IP of FLAG-CHIP efficiently brought down co-expressed GFP-SOX2, as well as endogenous HSP70 and HSP90 (Fig. 2C, left panel). However, while IP of GFP-SOX2 efficiently

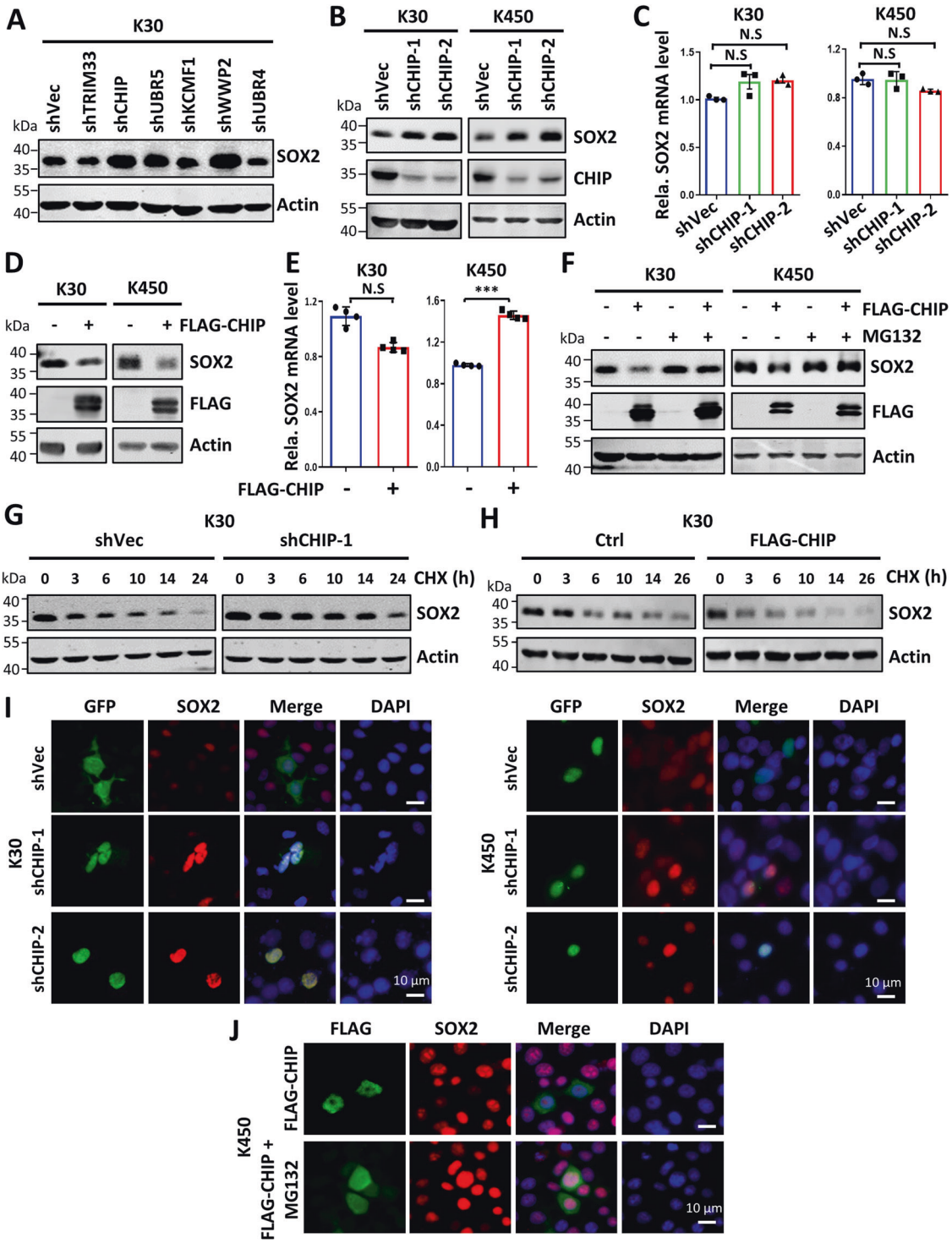

Fig. 1 CHIP negatively controls SOX2 protein level by promoting SOX2 proteasome degradation. A WB analysis showing the effect of knockdown of various ubiquitin E3 ligases on SOX2 protein levels in K30 cells. K30 cells were infected with lentiviral small hairpin RNAs (shRNAs) against different E3 ligases as indicated and cultured for three days before harvested for WB analysis. The effect of CHIP knockdown on SOX2 protein levels (**B**) and mRNA levels (**C**) in K30 and K450 cells. K30 and K450 cells were infected with two distinct lentiviral shRNAs against CHIP and cultured for three days before harvested for WB analysis (**B**) and quantitative RT-PCR analysis (**C**). The effect of ectopic overexpression of FLAG-CHIP on SOX2 protein levels (**D**) and mRNA levels (**E**) in K30 and K450 cells. K30 and K450 cells were transfected with FLAG-CHIP for two days before harvested for WB analysis (**D**) and quantitative RT-PCR analysis (**E**). **F** WB analysis showing that MG132 blocked SOX2 downregulation instigated by ectopic overexpression of FLAG-CHIP. K30 and K450 cells were transfected with or without FLAG-CHIP for two days, and MG132 was added at a concentration of 10 μg/ml 8 h before cells were harvested for WB analysis. **G**, **H** K30 cells were infected with lentiviral shVector or shCHIP for three days (**G**) or transfected with or without FLAG-CHIP (2 μg) and cultured for two days. K30 cells were then treated with CHX (100 μg/ml) at various times as indicated and subjected to WB analysis. **I** K30 and K450 cells were transfected with shCHIP plasmids for two days before being processed for immunofluorescent staining. **J** K450 cells were transfected with FLAG-CHIP (200 ng) for two days and treated with or without MG132 for 8 h before being processed for immunofluorescent staining. Different exposures applied to images in **I** and **J**.

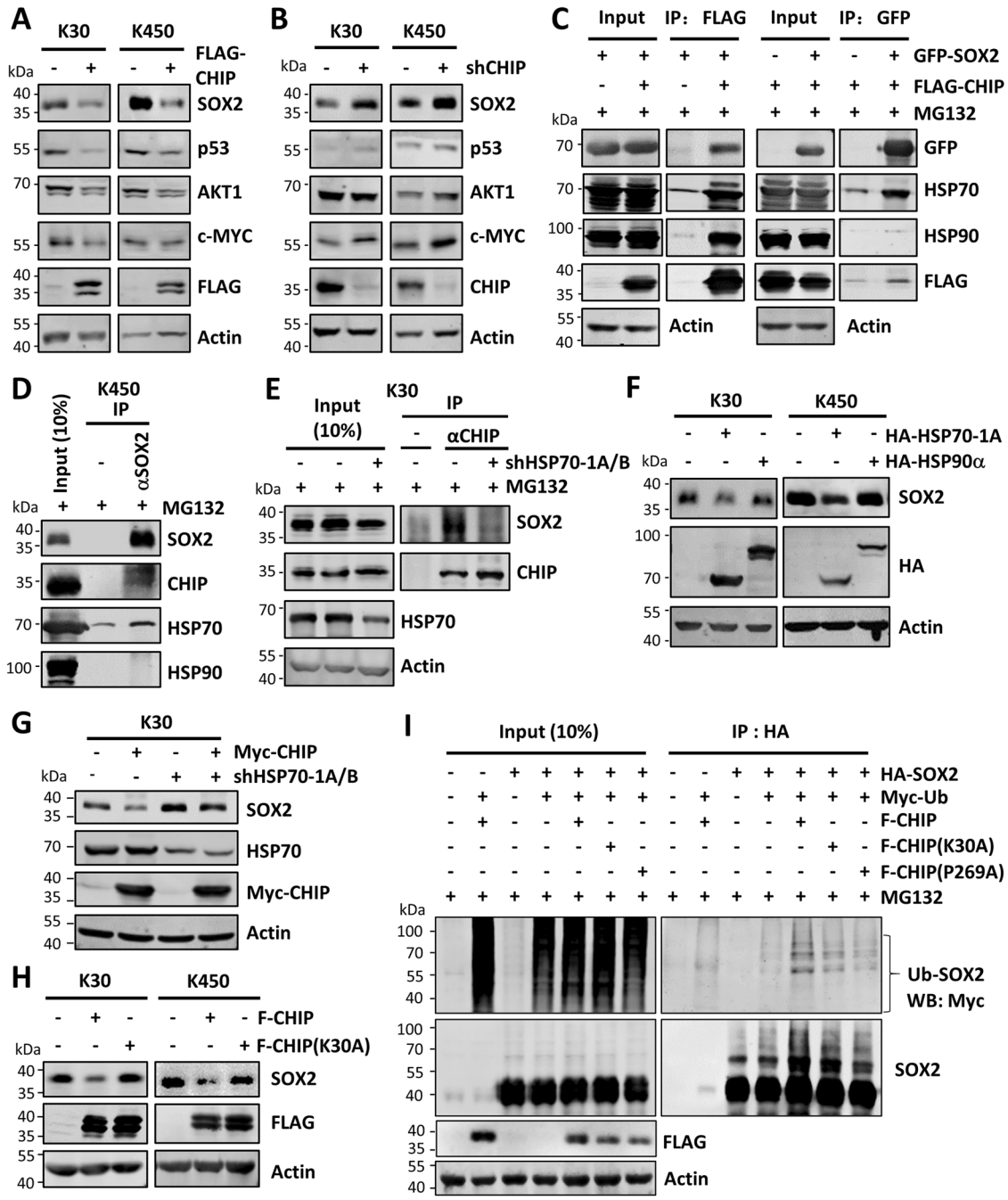

Fig. 2 HSP70 bridges the interaction between CHIP and SOX2 and is required for CHIP-mediated SOX2 ubiquitination and degradation. WB analysis showing the effect of ectopic overexpression of CHIP (**A**) or knockdown (**B**) on various CHIP client proteins. K30 and K450 cells were infected with lentiviral FLAG-CHIP or shCHIP and cultured for three days before harvested for WB analysis to detect the levels of SOX2, P53, AKT1 and c-MYC proteins. **C** IP-WB analysis for the interaction among SOX2, CHIP, HSP70, and HSP90 proteins. HEK293T cells were transfected with GFP-SOX2 and FLAG-CHIP plasmids as indicated for two days, and 10 μg/ml MG132 was added for 8 h before cells were harvested for IP with anti-FLAG or anti-GFP antibody and WB analysis using antibodies as indicated. **D** IP-WB analysis for the interaction among endogenous SOX2, CHIP, HSP70, and HSP90. Whole cell extracts were prepared from K450 cells and used for IP with anti-SOX2 antibody and WB using antibodies as indicated. **E** IP-WB analysis showing that knockdown of HSP70-1A/B impaired the interaction between SOX2 and CHIP in K30 cells. K30 cells were infected with lentiviral shRNA against both HSP70-1A and HSP70-1B as indicated for three days and subjected to treatment with 10 μg/ml MG132 for 8 h before harvested for IP-WB analysis. **F** WB analysis showing that ectopic expression of HSP70-1A but not HSP90α downregulated the level of SOX2. **G** WB analysis showing that knockdown of HSP70-1A/1B in K30 cells impaired CHIP-induced downregulation of SOX2. **H** WB analysis showing that ectopic expression of wild-type CHIP but not CHIP-K30A mutant downregulated the levels of SOX2 in K30 and K450 cells. F-CHIP(K30A), FLAG-CHIP(K30A). **I** IP-WB analysis showing that wild-type CHIP but not CHIP(K30A) or CHIP(P269A) mutants promoted SOX2 ubiquitination. HEK293T cell were transfected with plasmids as indicated for two days, and 10 μg/ml MG132 was added for 8 h before cells were harvested for denatured IP-WB analysis. F-CHIP, FLAG-CHIP; F-CHIP(K30A), FLAG-CHIP(K30A); F-CHIP(P269A), FLAG-CHIP(P269A).

brought down HSP70, only a small fraction of FLAG-CHIP and HSP90 was co-immunoprecipitated (Fig. 2C, right panel). Furthermore, while reciprocal co-IP experiments confirmed the interaction between endogenous CHIP and SOX2 in K450 cells (Fig. 2D and Supplementary Fig. S1A), this analysis also revealed that endogenous SOX2 interacted with HSP70 better than CHIP (Fig. 2D), raising the possibility that HSP70 may mediate the interaction between CHIP and SOX2. To test whether HSP70 mediates the interaction between CHIP and SOX2, we knocked down HSP70 in K450 cells and carried out co-IP assay with anti-CHIP antibody. As shown in Fig. 2E, knockdown of HSP70 markedly reduced the amount of SOX2 proteins co-immunoprecipitated with CHIP, suggesting that HSP70 most likely bridges the interaction between CHIP and SOX2. In agreement with this idea, we found that ectopic expression of HSP70-1A, one of the major subtypes of HSP70 family proteins [39], but not HSP90α facilitated the interaction between CHIP and SOX2 (Supplementary Fig. S1B). Furthermore, ectopic expression of HSP70-1A, but not HSP90α downregulated SOX2 protein level (Fig. 2F) and had no effect on SOX2 mRNA level (Supplementary Fig. S1C), whereas knockdown of HSP70-1A and HSP70-1B (HSP70-1A/B), two highly homologous major HSP70 subtypes by a single shRNA not only upregulated SOX2 protein level but also impaired SOX2 downregulation induced by ectopically expressed CHIP (Fig. 2G). Using a series of SOX2 deletion mutants (Supplementary Fig. S1D), the interaction with HSP70 was mapped to the C-terminal region of SOX2 (Supplementary Fig. S1E) and cycloheximide chase assay revealed that deletion of the C-terminal region promoted SOX2 protein stability (Supplementary Fig. S1F).

To further confirm that CHIP exerts SOX2 degradation in a HSP70-dependent manner, we made use of a CHIP(K30A) mutant that is defective in HSP70 interaction [40, 41]. Unlike wild-type CHIP, this mutant was unable to downregulate the levels of SOX2 proteins when ectopically expressed in both K30 and K450 cells (Fig. 2H). Furthermore, ubiquitination assay demonstrated that ectopic expression of wild-type CHIP but the CHIP(K30A) mutant promoted SOX2 ubiquitination (Fig. 2I). The ability for ectopically expressed CHIP to promote SOX2 ubiquitination was dependent on its E3 ligase activity, as ectopic expression of CHIP(P269A), a mutant defective in E3 ligase activity [42, 43], failed to enhance SOX2 ubiquitination (Fig. 2I). Together these results indicate that CHIP catalyzes SOX2 ubiquitination and proteasome-dependent degradation and that HSP70 is required for this process, most likely by bridging the interaction between CHIP and SOX2.

Both TPR and U-box domains are required for downregulation of SOX2 by CHIP

Having established that CHIP catalyzes SOX2 ubiquitination and degradation in a HSP70-dependent manner, we next analyzed the CHIP functional domains required for this process. CHIP has two major functional domains, namely the N-terminal tetratricopeptide repeat (TPR) domain, which allows CHIP to bind HSP70 and HSP90, and the C-terminal U-box E3 ligase domain (Fig. 3A) [40]. Consistent with aforementioned data that HSP70 is likely to mediate the interaction between CHIP and SOX2, we found that deletion of the TPR domain but not the U-box domain impaired the interaction between SOX2 and CHIP (Fig. 3B). In addition, both the TPR and U-box domains are required for CHIP to catalyze SOX2 ubiquitination (Fig. 3C) and down-regulate endogenous SOX2 proteins in both K30 and K450 cells (Fig. 3D). Furthermore, ectopic expression of either CHIP(K30A) mutant defective in HSP70 interaction or CHIP(P269A) mutant defective in E3 ligase activity failed to downregulate SOX2 in K30 and K450 cells (Fig. 3E). In fact, the ability for CHIP to downregulate SOX2 proteins was better illustrated by immunofluorescent staining of SOX2 proteins in FLAG-CHIP transfected cells (Fig. 3F). Although ectopically expressed wild-type FLAG-CHIP proteins were mainly localized in the cytoplasm, the FLAG-CHIP positive cells were essentially depleted of SOX2 proteins (Fig. 3F), demonstrating a robust activity of CHIP in targeting SOX2 degradation. Interestingly, while deletion of either TPR or U-box domain improved CHIP nuclear localization, it completely abolished CHIP's ability to downregulate SOX2 (Fig. 3F). Similarly, transfection of either CHIP(K30A) or CHIP(P269A) failed to downregulate SOX2. Furthermore, the cycloheximide chase assay revealed that all the CHIP mutants were inactive in downregulating SOX2 protein stability in K30 cells (Supplementary Fig. S2). Together these data support a working model that CHIP interacts with SOX2 through binding of HSP70 and catalyzes SOX2 ubiquitination and proteasome-dependent degradation through its intrinsic E3 ubiquitin ligase activity.

CHIP suppresses esophageal cancer cell proliferation and stem cell function

Given SOX2's prominent roles in cancer cell proliferation and stem cell function [3, 7, 9], we next examined whether CHIP regulates esophageal cancer cell proliferation and stem cell function. We found that ectopic overexpression of CHIP in K450 cells downregulated the level of endogenous SOX2 protein and moderately suppressed cell proliferation (Fig. 4A–C). Quantitative RT-PCR analysis revealed that ectopic overexpression of CHIP significantly downregulated the transcriptional levels of stem cell markers ALDH1, ALDH3, and CD44 [44, 45], suggesting ectopic overexpression of CHIP likely impaired the cancer stemness of K450 cells (Supplementary Fig. S3A). Indeed, by in vitro tumor sphere formation assay, we found that overexpression of CHIP substantially reduced the tumor sphere formation capability of K450 cells, suggesting that overexpression of CHIP significantly impaired cancer stem cell activity (Fig. 4D, E). Similar results were observed when these assays were performed with K30 cells (Supplementary Fig. S3B–E). In contrast, we found that knockdown of CHIP in K450 cells promoted cell proliferation and formation of tumor spheres, both in number and size (Fig. 4F–J). The ability for knockdown of CHIP to promote cell proliferation and tumor sphere formation was dependent on SOX2, as this activity was abrogated by simultaneous SOX2 knockdown (Fig. 4K–O). Thus, CHIP is likely to act as a tumor suppressor in esophageal cancer and does so at least in part through its ability to negatively regulate the level of SOX2 protein.

Inhibition of HSP90 Activity Induces SOX2 Degradation

For proteins that are targeted for degradation by CHIP, HSP90 often acts to promote protein stability [32]. Although ectopic expression of HA-HSP90 did not significantly affect the overall levels of SOX2 proteins in both K30 and K450 cells (Fig. 2F), we observed that inhibition of HSP90 by two different inhibitors, 17-allylamino-17-demethoxygeldanamycin (17-AAG) and 17-dimethylaminoethylamino-17-demethoxygeldanamycin (17-DMAG) [46], all led to a dose-dependent reduction of SOX2 protein in both K30 and K450 cells (Fig. 5A, B and Supplementary Fig. S4A). The inhibition of HSP90 in these experiments was manifested by a robust induction of HSP70 proteins, a hallmark of protein unfolding stress response (Fig. 5A, B and Supplementary Fig. S4A). Similarly, inhibition of HSP90 in mouse embryonic stem cells also resulted in marked downregulation of SOX2 (Supplementary Fig. S4B). Notably, the HSP90 inhibitor-induced downregulation of SOX2 protein is dependent on CHIP, because it was largely blocked when CHIP was knocked down by shRNA (Fig. 5C). The downregulation of SOX2 by HSP90 inhibitors is unlikely due to transcriptional repression of SOX2, because RT-qPCR analysis revealed that treatment with HSP90 inhibitors did not lead to a significant and consistent reduction of SOX2 mRNA (Fig. 5D). In agreement with the results of HSP90 inhibitors, we observed that knockdown of either HSP90α or HSP90β, two major HSP90 proteins by small RNA interference, resulted in downregulation of SOX2 in K450 cells (Fig. 5E). Due to marked sequence conservation between HSP90α or HSP90β, the antibody used recognized both forms of proteins. We

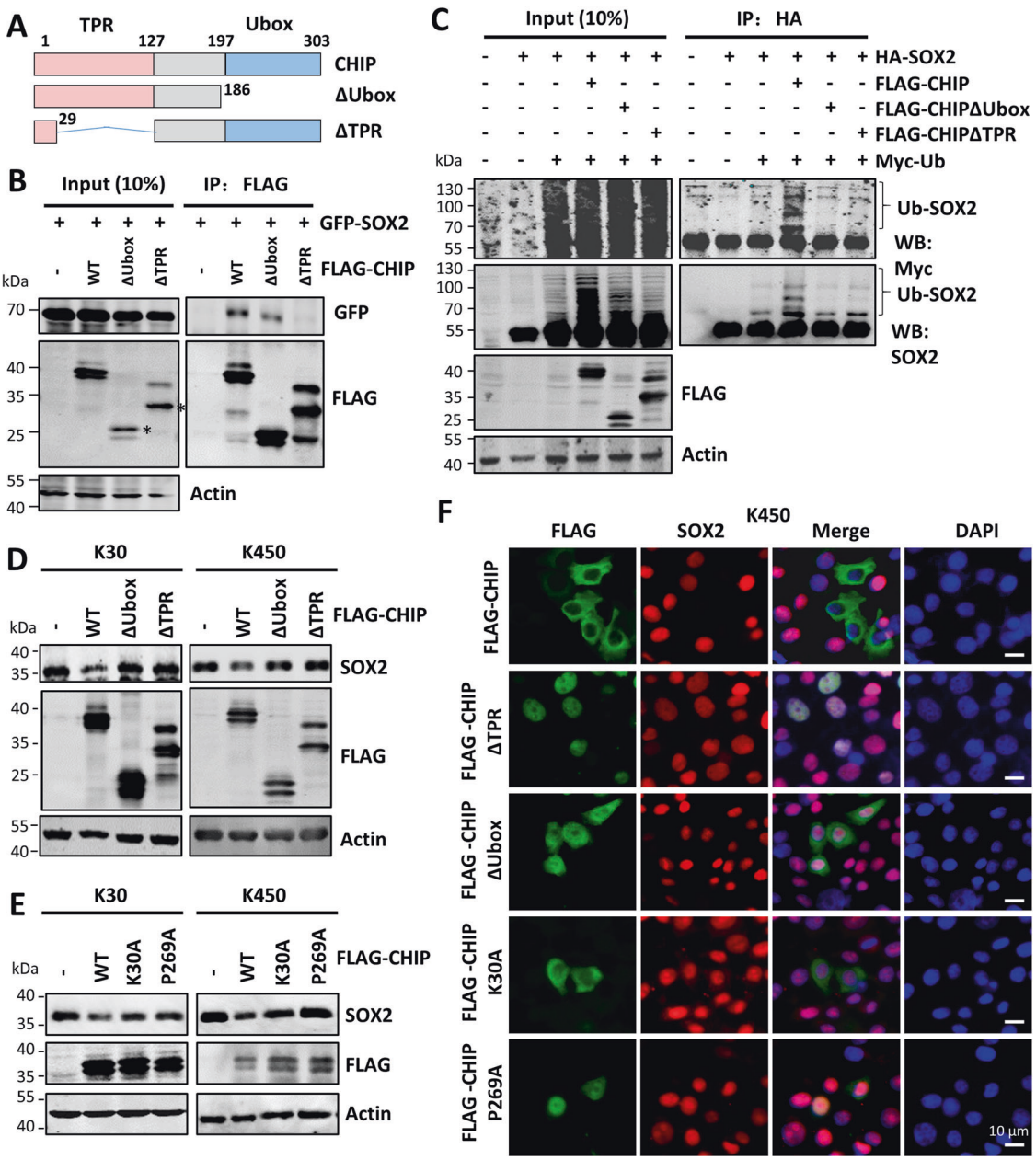

Fig. 3 Both TPR and U-box domains are required for downregulation of SOX2 by CHIP. A Diagram illustrating the structural and functional domains of full-length CHIP, CHIP-ΔTPR, and CHIP-ΔUbox deletion mutants. **B** IP-WB analysis examining the interaction of SOX2 with wild-type CHIP and mutants. GFP-SOX2 was co-transfected into HEK293T cells with FLAG-tagged wild-type or mutant CHIP (CHIP-ΔUbox or CHIP-ΔTPR) as indicated for two days. Cells were treated with 10 μg/ml MG132 for 8 h before harvested for IP-WB analysis. **C** IP-WB analysis showing that CHIP but not CHIP-ΔUbox or CHIP-ΔTPR mutant promoted the SOX2 ubiquitination. HEK293T cells were transfected with plasmids as indicated. Two days after transfection, 10 μg/ml MG132 was added for another 8 h before cells were harvested for denatured IP and WB analysis. **D** WB analysis showing that ectopic expression of wild-type CHIP, but not CHIP-ΔTPR or CHIP-ΔUbox mutant, downregulated the levels of SOX2 in K30 and K450 cells. **E** WB analysis showing the effect of ectopic expression of wildtype CHIP or mutants on SOX2 protein levels in K30 and K450 cells. **F** Immunofluorescent staining assay showing the effect of ectopic expression of wild-type CHIP or various mutants on the levels of SOX2 in K450 cells.

further confirmed that knockdown of HSP90α by shRNA resulted in reduction of SOX2 protein level (Supplementary Fig. S4C). In fact, a more impressive impact of HSP90α knockdown on downregulation of SOX2 protein was observed by immunofluorescent staining assay in K450 cells (Fig. 5F). Similarly, immunofluorescent staining assay revealed that HSP70-1A/B knockdown drastically upregulated SOX2 in K450 cells (Fig. 5F). To validate whether HSP90 inhibitors downregulate SOX2 by promoting SOX2 degradation, we compared SOX2 protein stability in K450 cells under the condition with or without HSP90 inhibitors. As shown in Fig. 5G, inhibition of HSP90 by both inhibitors markedly reduced the half-life of SOX2 proteins (from ~6 h to ~3 h). Furthermore, downregulation of SOX2 proteins by both HSP90 inhibitors was blocked by addition of MG132, suggesting that both inhibitors downregulate SOX2 via promoting proteasome degradation (Fig. 5H). In support of this idea, both HSP90 inhibitors were able to enhance SOX2 ubiquitination in a cell-based ubiquitination assay (Fig. 5I). Finally, we measured the effect of ectopic overexpression of HSP70-1A and HSP90α on SOX2 protein stability by

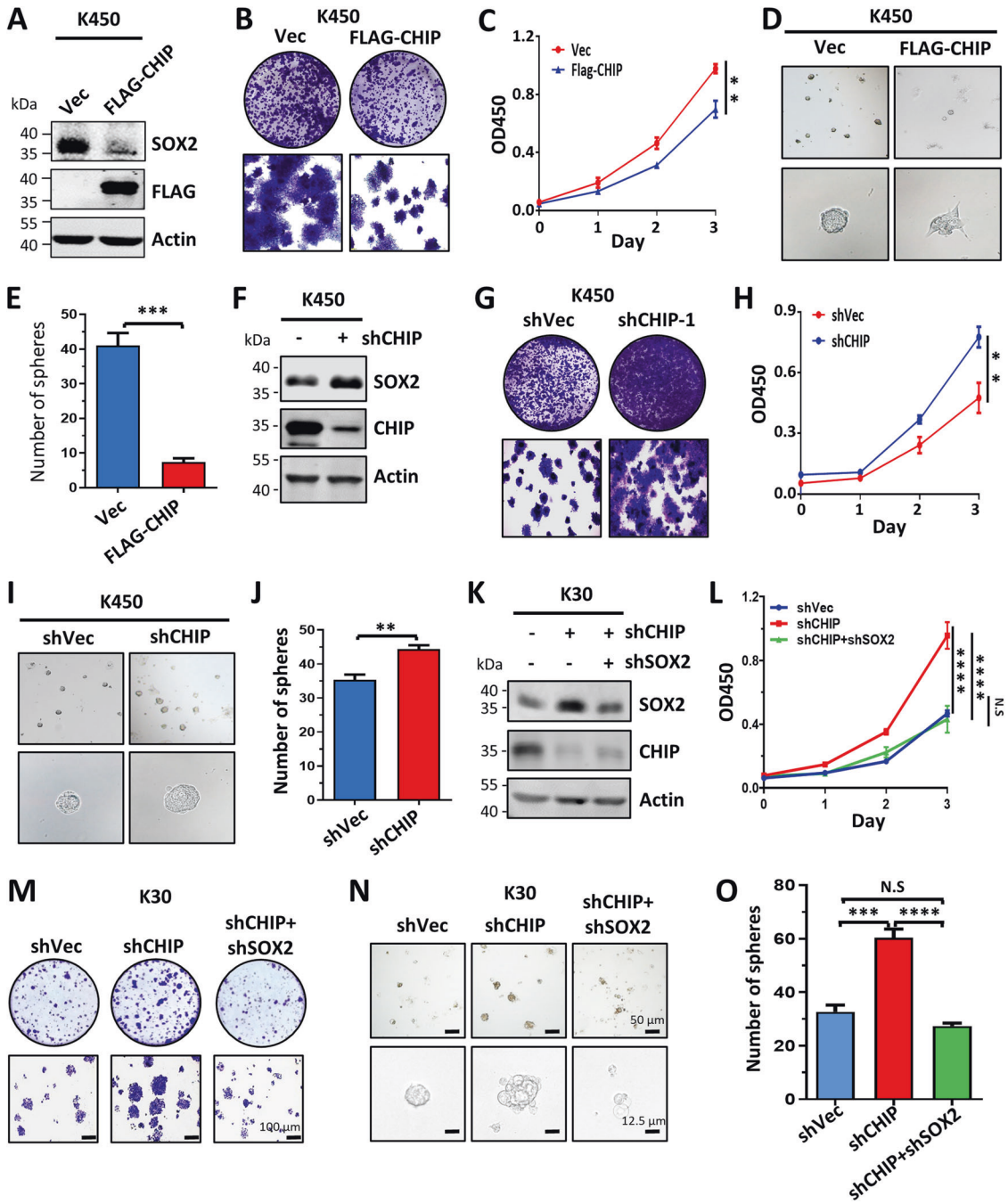

Fig. 4 CHIP suppresses esophageal cancer cell proliferation and stem cell function. A WB analysis showing stable overexpression of FLAG-CHIP markedly downregulated SOX2 in K450 cells. Stable FLAG-CHIP expressing K450 cells were generated by infection of K450 cells with lentiviruses expressing FLAG-CHIP. Stable overexpression of FLAG-CHIP impaired K450 cell colony formation (**B**), cell proliferation (**C**), and tumor sphere formation (**D** and **E**). **F** WB analysis showing stable knockdown of CHIP upregulated SOX2 protein level in K450 cells. K450 cells with stable CHIP knockdown were generated by infection of K450 cells with lentiviruses expressing FLAG-CHIP. Knockdown of CHIP promoted K450 cell colony formation (**G**), proliferation (**H**), and tumor sphere formation (**I** and **J**). **K** WB analysis showing the levels of SOX2 in CHIP knockdown and CHIP/SOX2 double knockdown K30 cells. Knockdown of SOX2 abolished CHIP knockdown-instigated increase of K30 cell proliferation (**L**), colony formation (**M**), and oncosphere formation (**N** and **O**).

cycloheximide chase assay. The representative results in Fig. 5J showed that ectopic overexpression of HSP70-1A markedly reduced, whereas ectopic overexpression of HSP90α enhanced, SOX2 protein stability. Taken together, these data reveal a role of HSP90 chaperone in antagonizing CHIP/HSP70-instigated SOX2 degradation. In addition, these data render HSP90 inhibitors as potential therapeutic agents for SOX2-positive ESCC cancers.

CHIP is predominantly localized in the cytoplasm in esophageal tumors

To investigate whether regulation of SOX2 by CHIP is of pathological relevance, we first analyzed the expression data of CHIP and SOX2 from The Cancer Genome Atlas (TCGA) clinical esophageal cancer samples, including both esophageal adenocarcinoma and squamous carcinoma. This analysis revealed that while SOX2 was significantly upregulated in esophageal squamous carcinoma samples, CHIP was

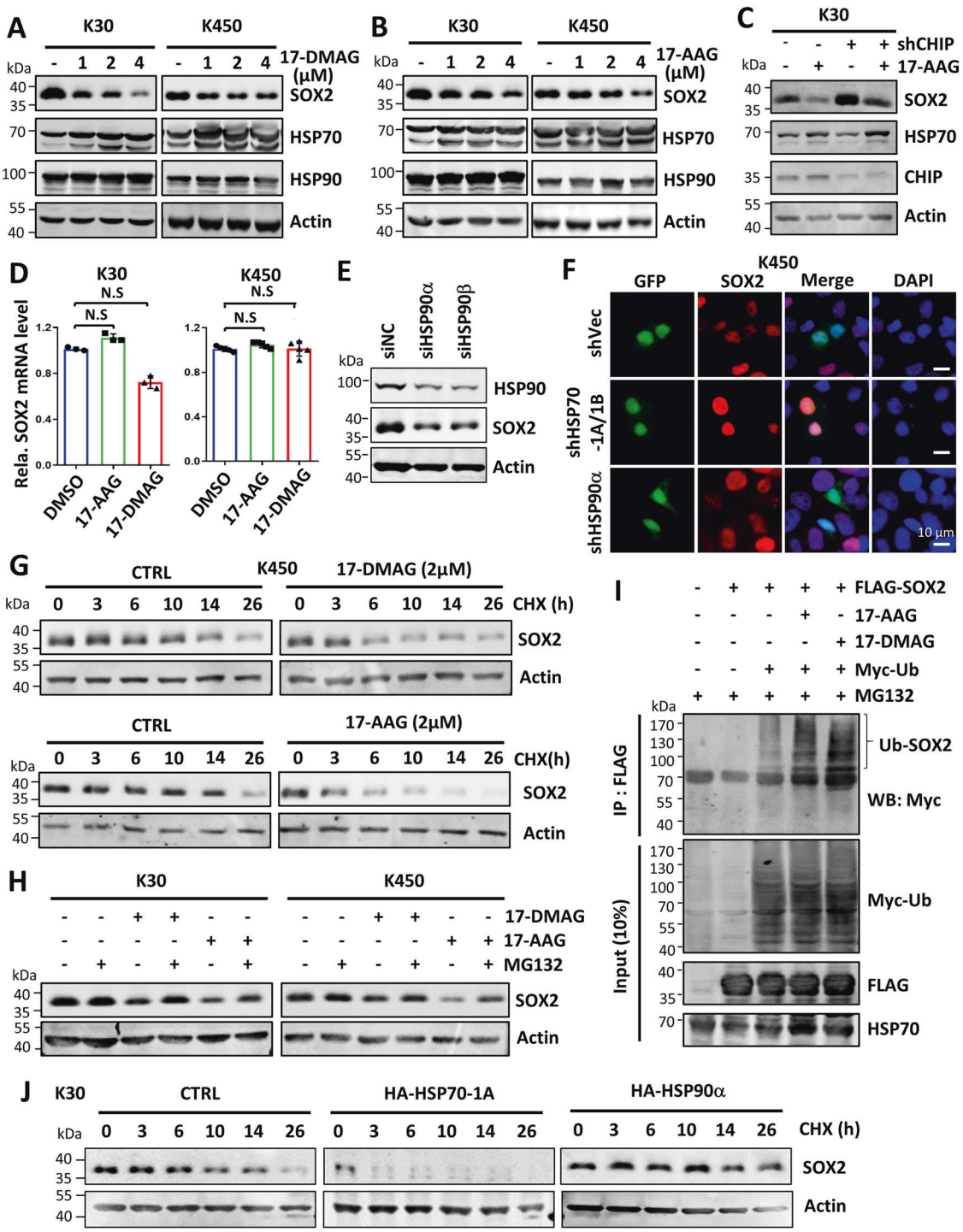

only slightly upregulated (Supplementary Fig. S5A, B). To examine the levels of CHIP and SOX2 proteins in esophageal squamous carcinomas and adjacent normal tissue specimens, we carried out tissue microarray analysis. In total, 266 esophageal squamous carcinomas and 84 adjacent normal tissues passed quality control test and were further analyzed. Consistent with previous studies [18, 25], SOX2 was hardly detected in adjacent normal tissues and was readily detected in tumor specimens (Fig. 6A, B). CHIP was clearly detected in both tumors and adjacent normal tissues, with varied degrees of expression (Fig. 6C, D). Overall, no significant difference was detected statistically in terms of the levels of CHIP proteins between adjacent normal tissues, hyperplasia, dysplasia and carcinoma (Fig. 6D). However, a striking difference in subcellular localization was noted for CHIP between adjacent normal tissues and esophageal carcinomas (Fig. 6E). Whereas CHIP was often observed as both cytoplasm and nuclear localization in most normal tissues and relative strong nuclear staining in some cases, it was predominantly detected in the cytoplasm in esophageal carcinomas (Fig. 6C, E). Subcellular fractionation experiments with K30 and K450 esophageal cancer cell lines confirmed that CHIP was predominantly localized in the cytoplasm fraction, whereas SOX2 was mainly localized in the nuclear fraction (Fig. 6F). Both HSP70 and HSP90 were mainly detected in the cytoplasm fraction, consistent with them being predominantly cytoplasmic proteins.

Fig. 5 Inhibition of HSP90 activity induces SOX2 degradation. WB analysis showing that treatment with HSP90 inhibitors 17-DMAG (**A**) or 17-AAG (**B**) resulted in a dose-dependent downregulation of SOX2 in K30 and K450 cells. K30 and K450 cells were treated with an increasing concentration of 17-DMAG or 17-AAG for 24 h. Note inhibition of HSP90 resulted in marked elevation of HSP70 protein levels. **C** WB analysis showing that knockdown of CHIP abrogated HSP90 inhibitor 17-AAG-induced SOX2 downregulation. K30 cells were infected with or without lentiviral shRNA against CHIP for three days and then treated with or without 2 μM 17-AAG for 24 h before harvested for WB analysis. **D** Quantitative RT-PCR analysis showing the effect of treatment with HSP90 inhibitors 17-DMAG and 17-AAG on the levels of SOX2 mRNA in K30 and K450 cells. The cells were treated with or without 2 μM 17-DMAG or 17-AAG as indicated. **E** WB analysis showing that knockdown of either HSP90α or HSP90β downregulated SOX2 protein level in K450 cells. **F** Immunofluorescent staining showing the effect of knockdown of either HSP70 or HSP90 on SOX2 protein levels. K450 cells were transiently transfected with plasmids encoding shHSP70-1A/B or shHSP90α for two days before processed for immunofluorescent staining. The shRNA vector also encodes GFP. **G** Protein stability assay showing that 17-DMAG and 17-AAG treatment markedly reduced the half-life of SOX2 proteins in K450 cells. K450 cells were treated with CHX (100 μg/ml) and with or without 2 μM 17-DMAG (top panel) or 17-AAG (bottom panel) respectively as indicated. **H** WB analysis showing that MG132 treatment blocked SOX2 downregulation induced by 2 μM 17-DMAG and 17-AAG. K30 and K450 cells were treated with 2 μM 17-DMAG or 17-AAG for 24 h, and 10 μg/ml MG132 was then added for 8 h before cells were harvested for WB analysis. **I** IP-WB analysis showing that inhibition of HSP90 activity resulted in elevated ubiquitination on SOX2. HEK293T cells were transfected with plasmids as indicated. Cells were then treated with or without 2 μM 17-DMAG and 17-AAG respectively for 24 h, and 10 μg/ml MG132 was added for 8 h before cells were harvested for denatured IP and WB analysis. **J** Cycloheximide chase assay showing the effect of ectopic expression of HSP70-1A or HSP90α on SOX2 protein stability.

As a potential explanation of CHIP nuclear exclusion in esophageal squamous carcinomas, we analyzed the expression of exportin-1/CRM-1 in normal tissues, esophageal adenocarcinoma, and squamous cell carcinoma in TCGA database. This analysis revealed elevated expression of exportin-1/CRM-1 in both esophageal adenocarcinoma and squamous cell carcinoma (Fig. 6G). We further confirmed by Western blot analysis the elevated levels of exportin-1/CRM-1 protein in seven paired adjacent normal tissues and esophageal squamous carcinoma (Fig. 6H). Thus, elevated exportin-1/CRM-1 proteins may drive CHIP nuclear export in esophageal cancer.

To test if CHIP-mediated SOX2 degradation regulates ESCC tumorigenesis, we established a K450 cell line that stably expressed FLAG-CHIP and confirmed that expression of FLAG-CHIP resulted in diminished SOX2 protein level (Fig. 6I). Furthermore, RT-qPCR analysis revealed that the expression of FLAG-CHIP downregulated the expression of four representative SOX2 target genes (Supplementary Fig. S5C, D). In contrast, knockdown of CHIP elevated the expression of the same set SOX2 target genes (Supplementary Fig. S5E), confirming that manipulating CHIP expression can influence SOX2 transcriptional activity and function. In addition, expression of FLAG-CHIP sensitized K450 cells to inhibition of cell proliferation by chemotherapeutic agent carboplatin (Supplementary Fig. S5F). Subsequent tumor xenograft assay in nude mice showed that expression of FLAG-CHIP significantly retarded tumor progression of K450 cells (Fig. 6J, K). RT-qPCR analysis revealed reduced expression of ALDH1, ALDH3, and CD44 in xenografted tumors derived from FLAG-CHIP expressing K450 cells (Supplementary Fig. S6). Together these results suggest that CHIP can act as a tumor suppressor in ESCC by downregulating SOX2 and its associated cancer stemness.

CHIP targets SOX2 ubiquitination and degradation in the nucleus

Although CHIP is generally considered to target misfolded proteins for ubiquitination and degradation in the cytoplasm as a mechanism of protein quality control [31, 32], our findings that CHIP is by and large depleted in the nucleus of esophageal tumor cells and that SOX2 is broadly overexpressed in esophageal tumors raised a question whether diminished nuclear CHIP could contribute to SOX2 overexpression in esophageal tumors. We thus decided to investigate whether CHIP targets SOX2 degradation in the nucleus and/or in the cytoplasm. To this end, we treated K450 cells with leptomycin B (LMB), an inhibitor that suppresses CRM-1-dependent nuclear export. We found that LMB treatment resulted in increased nuclear accumulation of CHIP (Fig. 7A, B), indicating that CHIP is dynamically shuttered between the nucleus and cytoplasm. Notably, LMB treatment also resulted in downregulation of SOX2 protein level (Fig. 7A). Importantly, LMB-induced SOX2 downregulation was blocked by addition of MG132 (Fig. 7C) and by knockdown of CHIP (Fig. 7D), indicating that LMB induced SOX2 downregulation via proteasome degradation and it was dependent on CHIP. Consistent with this idea, we found that LMB treatment markedly reduced SOX2 protein stability (Fig. 7E). Furthermore, subcellular fractionation experiments in Fig. 7F showed that CHIP enhanced SOX2 ubiquitination primarily in the nuclear fraction. Together, these data suggest a working model that it is the nuclear CHIP that targets SOX2 for ubiquitination and proteasome-dependent degradation (Fig. 7G, H).

DISCUSSION

Accumulative evidence supports aberrant SOX2 expression as a causal determinant for squamous cell carcinomas including esophageal cancer [5–11]. Exploring the molecular mechanisms leading to SOX2 overexpression in cancer is therefore essential not only for cancer etiology, but also for better therapeutic strategies against cancer. Here we uncovered that in esophageal cancer cells SOX2 is oppositely regulated by CHIP/HSP70 and HSP90. While HSP90 stabilizes SOX2 (Fig. 5), CHIP/HSP70 target SOX2 for ubiquitination-dependent proteasome degradation (Figs. 1–4). We provided evidence that CHIP nuclear export is likely a mechanism contributing to broad SOX2 overexpression in esophageal squamous carcinoma (Figs. 6 and 7) and that HSP90 inhibitors are potential therapeutic agents for SOX2-dependent esophageal squamous carcinoma (Fig. 5).

As a transcription factor with potent function in embryonic development, differentiation, tissue homeostasis and cell fate reprogramming [1–4], the SOX2 dosage must be tightly controlled, as both elevated and reduced levels of SOX2 have been shown to impair embryonic stem cell self-renewal and function [47]. Besides gene amplification and transcriptional regulation, protein turnover is a key mechanism that ultimately determines the cellular SOX2 dosage. A few ubiquitin enzymes including WWP2, CUL4A, UBR5, CRL4(DCAF5) and Ube2s have been shown to target SOX2 for ubiquitination and proteasome degradation [26, 29, 30, 48–50], and AKT has been shown to stabilize SOX2 in embryonic stem cells [27], esophageal cancer cells [29], and large B cell lymphoma [51] by antagonizing SOX2 ubiquitination and proteasome degradation. Thus, our identification of CHIP as a ubiquitin E3 that targets SOX2 for degradation in ESCC cells further underscores the physiological significance of SOX2 dosage control. In support of our finding, a recent study reported that CHIP maintains SOX2 proteostasis in embryonic stem cells [48]. While our multiple lines of evidence support a role of CHIP and its associated HSP70 chaperone in targeting SOX2 degradation, it is noteworthy that this is not equivalent to the routine protein quality control process that selectively targets unfolded or misfolded nascent polypeptides for degradation in cytosol.

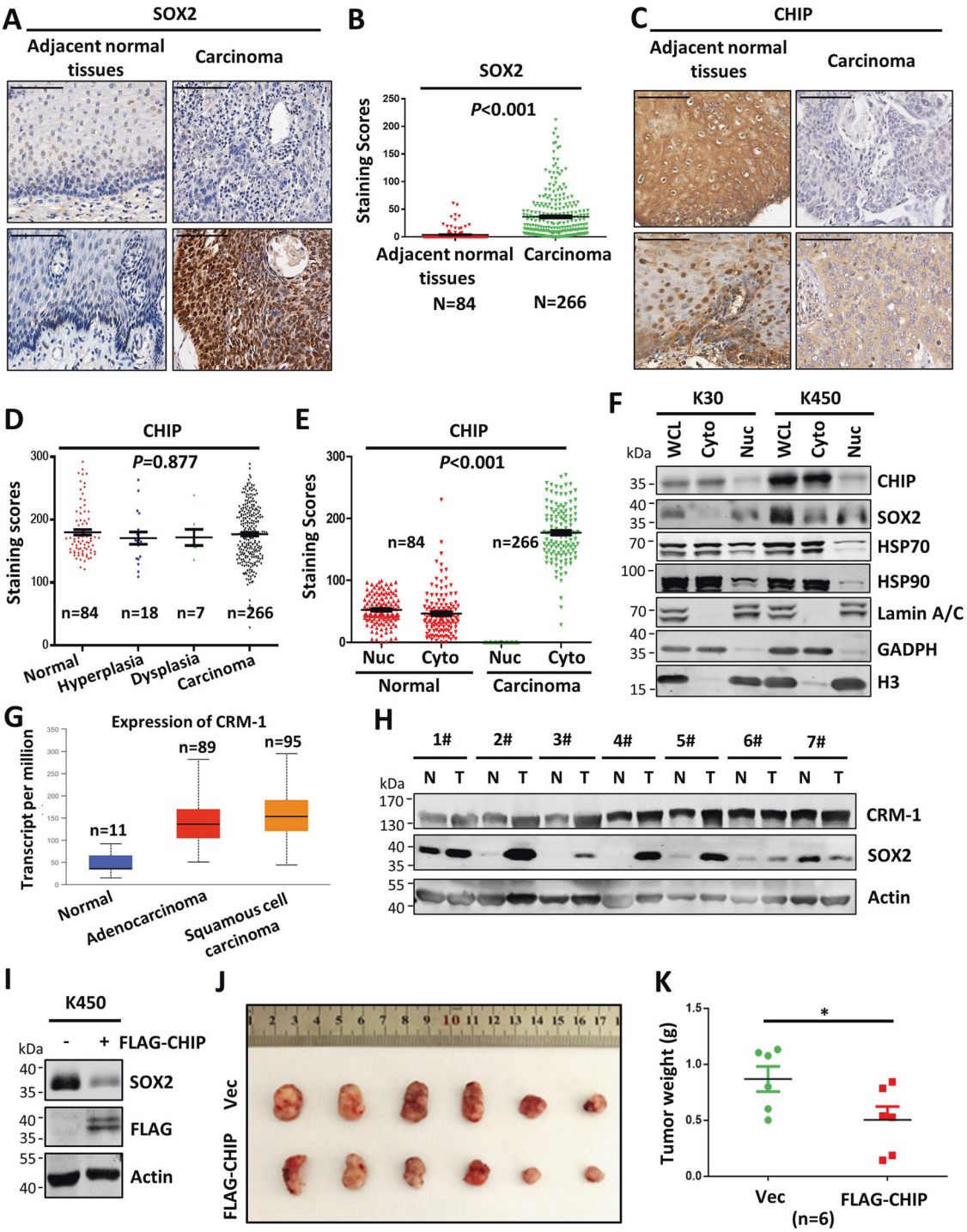

Fig. 6 CHIP is predominantly localized in the cytoplasm in esophageal tumors. A IHC staining of SOX2 in representative ESCC tumors and paired adjacent normal tissues from ESCC tissue microarrays. **B** Scatter plots of SOX2 levels in tissue microarrays of ESCC tumors and adjacent normal tissues. **C** IHC staining of CHIP in representative ESCC tumors and paired adjacent normal tissues from ESCC tissue microarrays. **D** Scatter plots of CHIP levels in tissue microarrays of ESCC tumors and adjacent normal tissues. **E** Scatter plots of nuclear and cytoplasmic CHIP levels in tissue microarrays of ESCC tumors and adjacent normal tissues. **F** WB analysis of CHIP subcellular localization in K30 and K450 cells. GAPDH, cytosol marker; Lamin A/C, nuclear marker; histone H3, chromatin marker. Note that CHIP was predominantly detected in the cytoplasm, whereas SOX2 was primarily localized in the nucleus. **G** The levels of exportin-1/CRM-1 transcripts in the normal esophageal tissues, adenocarcinoma, and squamous carcinoma available in TCGA database. **H** WB analysis of CRM-1 and SOX2 in seven paired adjacent normal esophageal tissues and esophageal squamous carcinoma. N, adjacent normal esophageal tissues; T, esophageal squamous carcinoma. **I** WB analysis showing stable expression of FLAG-CHIP downregulated SOX2 protein level in K450 cells. The images of xenografted tumors (**J**) and the weights of xenografted tumors (**K**) of control and K450 cells with stable expression of FLAG-CHIP.

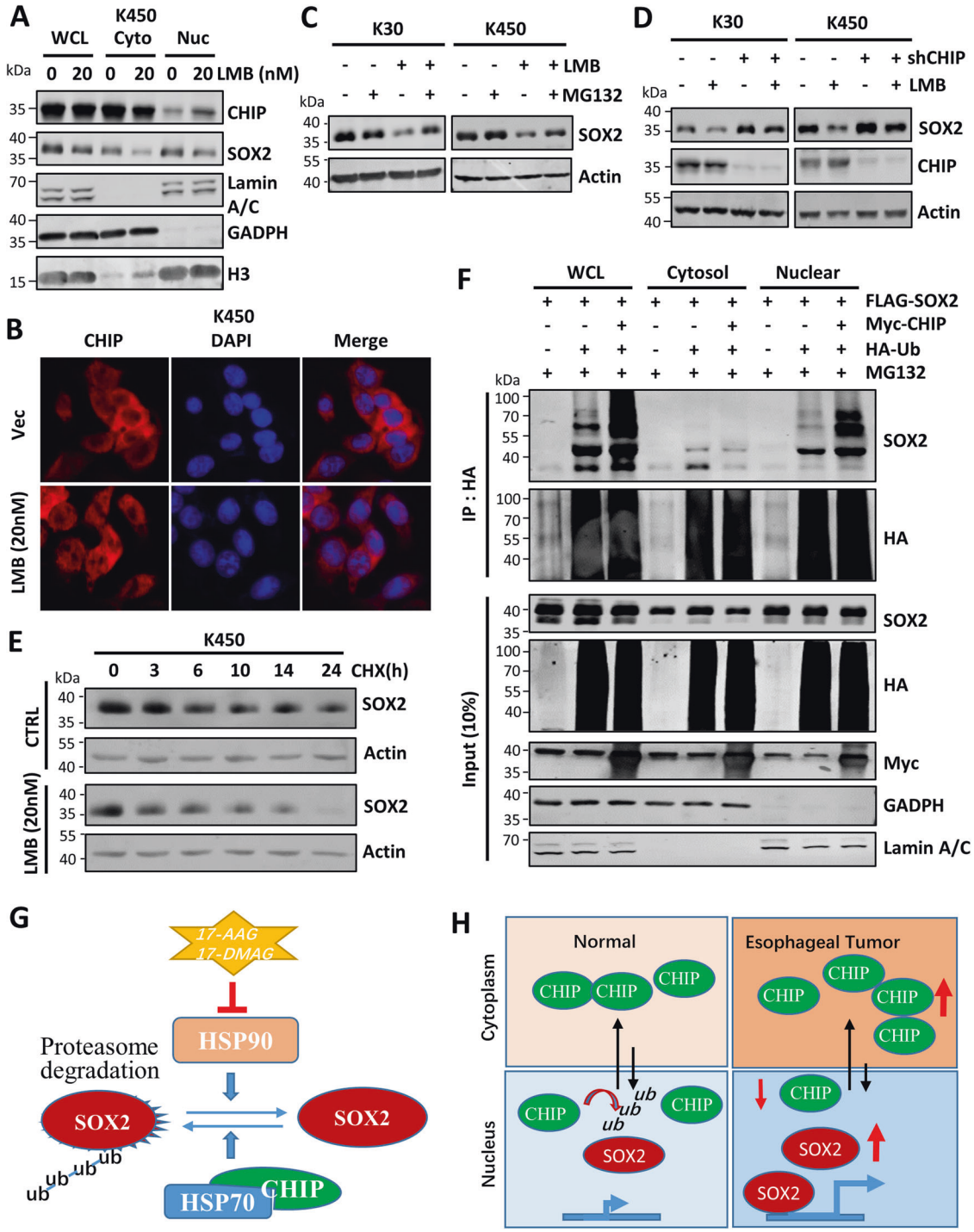

Fig. 7 CHIP targets SOX2 ubiquitination and degradation in the nucleus. A WB analysis showing that leptomycin B (LMB) treatment increased the level of nuclear CHIP. K450 cells treated with 20 nM LMB for 24 h before being subjected to subcellular fractionation and WB analysis. **B** Immunofluorescent staining analysis showing increased nuclear CHIP in K450 cells upon LMB treatment. **C** WB analysis showing that LMB treatment downregulated SOX2 protein level and addition of MG132 blocked LMB-induced SOX2 downregulation. K30 and K450 cells were treated with 20 nM LMB for 24 h, and MG132 was added at 10 μg/ml 8 h before cells were harvested for WB analysis. **D** WB analysis showing that knockdown of CHIP impaired LMB-induced SOX2 downregulation. K30 and K450 cells were infected with or without shCHIP for three days and then treated with or without 20 nM LMB for 24 h before being harvested for WB analysis. **E** Cycloheximide chase assay showing that LMB treatment markedly reduced the half-life of SOX2 proteins in K450 cells. **F** IP-WB analysis showing that CHIP primarily catalyzed the ubiquitination of nuclear SOX2. HEK293T cells were transfected with FLAG-SOX2, HA-Ub and Myc-CHIP as indicated. Two days after transfection, 10 μg/ml MG132 was added for another 8 h before cells were harvested for IP-WB analysis. **G** Schematic diagram showing that SOX2 is a novel substrate of CHIP E3 ligase. SOX2 is stabilized by HSP90, possibly by its ability to promote proper protein folding, and targeted for ubiquitination and degradation by CHIP/HSP70. Inhibition of HSP90 by 17-AAG and 17-DMAG is likely to enhance SOX2 degradation by increasing HSP70 protein level as well as misfolded SOX2 protein level. **H** A working model illustrating that aberrant CHIP cytoplasmic localization is a mechanism for elevated SOX2 protein level in esophageal tumor cells. Elevated SOX2 expression is a key oncogenic determinant of esophageal squamous carcinoma.

Instead, we showed that CHIP selectively targets SOX2 proteins for ubiquitination and degradation in the nucleus, implying that it acts on mature SOX2 proteins. However, because HSP70 is required for CHIP to interact with and target SOX2 for ubiquitination and degradation, it remains unclear if this process is selective for native mature SOX2 and/or misfolded SOX2. One plausible scenario is that SOX2 is a structurally unstable or flexible protein (as most potent transcription factors) and undergoes folding and unfolding constantly. HSP70 and CHIP then sense unfolded/misfolded SOX2 and target them for degradation. Alternatively, HSP70 and CHIP interact with and target native SOX2 proteins for ubiquitination and degradation. We favor the first model, because we found that inhibition of HSP90 drives SOX2 ubiquitination and degradation in a CHIP-dependent manner (Fig. 5). As HSP90 chaperone is well known for its function in promoting protein folding [32, 46], HSP90 is likely to enhance SOX2 stability by promoting SOX2 refolding. This working model, as illustrated in Fig. 7G, fits with our finding that HSP70 and CHIP mainly target SOX2 degradation in the nucleus, because unfolded nascent protein is only expected to be present in cytosol. In this regard, a growing number of nuclear proteins have been identified as substrates for CHIP-mediated ubiquitination and degradation [38, 52–54], although very few have been unambiguously tested if this process occurs in the nucleus.

An interesting observation in our study is that CHIP is predominantly cytoplasm localized and essentially absent in the nucleus in esophageal squamous tumor cells (Fig. 6C, E). In most control normal tissues, CHIP was detected in both cytoplasm and nuclear compartments (Fig. 6C, E). In search of potential explanation for the observed CHIP nuclear exclusion, we noticed elevated expression of exportin-1/CRM-1 in esophageal tumors both in the levels of mRNA and protein (Fig. 6G, H). Thus, we suggest that elevated expression of exportin-1/CRM-1 may drive CHIP nuclear export in esophageal cancer cells (Fig. 7H). Given CHIP as a chaperone-associated E3 ligase, we also investigated whether HSP70 and HSP90 regulate CHIP subcellular localization. Our preliminary study revealed that HSP70 and HSP90 regulate neither CHIP expression nor its subcellular localization in esophageal cancer cell lines (Supplementary Fig. S7). Thus, the underlying mechanism(s) for altered CHIP subcellular localization in esophageal tumors is currently incompletely understood and warrants for further investigation.

We presented evidence that CHIP catalyzes SOX2 ubiquitination and degradation mainly in the nucleus compartment. The observation that CHIP is mainly cytoplasm localized in esophageal squamous tumors promoted us to investigate whether altered CHIP subcellular localization could contribute to aberrant SOX2 overexpression in esophageal cancer cells. Our data indeed demonstrate that treatment with LMB to block exportin-1/CRM-1 mediated nuclear export resulted in elevated CHIP nuclear accumulation, increased SOX2 ubiquitination and downregulation of SOX2 proteins (Fig. 7). This data thus supports a working model in Fig. 7H that CHIP catalyzes SOX2 ubiquitination and degradation mainly in the nucleus compartment. However, because LMB treatment is likely to cause mislocalization of many proteins, it is formally possible that the accumulation of other E3 ligases may also contribute to enhanced SOX2 downregulation upon LMB treatment.

In summary, in this study we uncover a critical role for CHIP and HSP70 and HSP90 chaperones in control of SOX2 stability and dosage. CHIP and HSP70 act together to ubiquitinate and target SOX2 for proteasome degradation, whereas HSP90 protects SOX2 from CHIP-induced degradation. Accelerated CHIP nuclear export is likely a mechanism for SOX2 overexpression in esophageal tumor cells. HSP90 inhibitors are warranted for exploration as therapeutic agents for various SOX2-positive cancers including esophageal squamous carcinoma.

MATERIALS AND METHODS

Plasmids construction

CHIP coding region was subcloned into FLAG/Myc-tagged pCDH vector. HSP70-1A and HSP90α coding regions were subcloned into HA-tagged pCDNA3.1-vector. SOX2 expression constructs were as described [29]. The Ubox deletion construct (Δ Ubox) deleted the region spanning amino acids 186 to 303, whereas the TPR deletion mutant (ΔTPR) deleted the region spanning amino acids 29 to 127. All mutants were generated by PCR-based point or truncation mutagenesis strategy and verified by DNA sequencing.

To generate shRNA constructs against human SOX2, CHIP, HSP70-1A/B, HSP90α, TRIM33, UBR5, KCMF1, WWP2 and UBR4 genes, the corresponding shRNA oligonucleotides were cloned either into pLKO.1-GFP vector for transient transfection or pLKO.1-puro for stable knockdown as described [29]. The resulting constructs were sequencing-verified. The sequences for shRNAs are listed in Supplementary Table S1.

Cell transfection and stable cell line establishment

Human esophagus squamous carcinoma Kyse30 (K30 hereafter) cells and human embryonic kidney HEK293T cells were cultured with DMEM medium (Gibco) containing 10% fetal calf serum (Gibco) and 100 U/ml penicillin/streptomycin solution (Gibco). Human esophagus squamous carcinoma Kyse450 (K450 hereafter) cells were cultured with RPMI-1640 medium (Invitrogen) containing 10% fetal calf serum and 100 U/ml penicillin/streptomycin solution. All cell lines were cultured at 37 °C in a humidified atmosphere containing 5% CO_2. Transient transfection was performed using LipoFiter (Hanbio) according to the manufacturer's instructions.

For stable cell line generation, lentiviruses were produced by LipoFiter transfection of HEK293T cells with pLKO.1-puro- shRNA plasmids or pCDH expression plasmids and helper plasmids pMD2.G and psPAX2. Viral supernatants were collected 48 h after transfection and filtered through a 0.22 mm filter. The collected lentiviruses were used to infect desired cell lines according to the manufacturer's protocol. 12 h after infection, the medium was replaced with the corresponding complete medium. After 24 h, the cells were cultured with the medium containing 1 μg/ml puromycin (Sigma-Aldrich) for 1 week to screen for stably transfected cell lines.

Antibodies and inhibitors

The following antibodies were used in this study: SOX2 (Abcam, #97959), CHIP (SAB, #49933), HSP70 (Proteintech, #10995-1-AP), HSP90 (Proteintech, #13171-1-AP), AKT (Absci, #abs4582), Lamin A/C (Abcam, #ab133256), GAPDH (Abmart, #M20006L), CRM1 (Proteintech, #66763-1-lg), histone H3 (Abcam, #ab1791), β-actin (HUABIO, #M1210-2), FLAG (Sigma, #F1804), HA (Abmart, #M20003), Myc (Abmart, #M20002), p53 (Santa Cruz, #sc-126), and GFP (Abmart, #M2004L). The following secondary antibodies were used: Alexa Fluor 680 goat anti-rabbit IgG (Jackson ImmunoResearch, #111-625-144), Alexa Fluor 790 goat anti-mouse IgG (Jackson ImmunoResearch, #115-655-146), Alexa Fluor 594 goat anti-rabbit IgG (Jackson ImmunoResearch, #111-585-003), and Alexa Fluor 488 goat anti-mouse IgG (Jackson ImmunoResearch, #115-545-003).

Leptomycin B (#HY-16909) and HSP90 inhibitors 17-AAG (#HY-10211) and 17-DMAG (#HY-10389) were purchased from MCE.

Western blot, immunofluorescence staining and co-immunoprecipitation

Western blot (WB), immunofluorescence and co-immunoprecipitation were performed essentially as described [27, 29, 38].

In vivo ubiquitination assay

To analyze SOX2 ubiquitination catalyzed by CHIP and various CHIP mutants in vivo, HEK293T cells were transfected with various expression constructs as indicated. Two days after transfection, the resulting cells were treated with 10 μg/ml MG132 for 8 h before harvested for IP-WB analysis under denaturing condition. In brief, after washing with PBS once, cells were directly lysed using denaturing lysis buffer (150 mM NaCl, 0.1% NP40 or Triton X-100, 25 mM Tris-HCl, pH 8.0, 5 mM EDTA, 10% glycerol and 1% SDS) and heated at 100 °C for 20 min to inactivate the deubiquitinating enzymes. Lysates were cleared by centrifugation at 12000 rpm for 20 min and diluted with denaturing binding buffer without SDS to a final SDS concentration of 0.1% before subjected to WB or IP-WB analysis using antibodies as indicated.

cDNA preparation and quantitative RT-PCR

For quantitative RT-PCR (RT-qPCR), total RNAs were extracted from indicated cell lines using the TRIzol-based method, and cDNA was prepared with the ReverTra Ace qPCR RT Kit (TOYOBO) by following the manufacturer's protocol. The cDNAs were then used for RT-qPCR through CFX96 Touch™ Deep Well Real-Time PCR. Primers for RT-PCR sequences are listed in Supplementary Table S1.

Cycloheximide chase assay

Cycloheximide (CHX) chase assay was performed to determine the half-life of SOX2 proteins as described [29].

Subcellular fractionation

To separate cell extracts into the cytosol and nuclear fractions, cells were washed with cold 1×PBS twice and resuspended with 250 µl Buffer A (10 mM Hepes-NaOH, pH 7.9, 10 mM KCl, 1.5 mM $MgCl_2$, and 0.5 mM β-Mercaptoethanol) and incubated on ice for 15 to 20 min. NP-40 was added to a final concentration of 0.1%, and the cell suspensions were vortexed and incubated on ice for 5 to 10 min. The cell extracts were centrifuged at 1000 rpm for 5 min and the resulting supernatants were designated as cytosols. The nuclear pellets were washed with cold 1×PBS three times and then treated as nuclear fractions.

Cell proliferation assay

Cells indicated were counted and plated in 96-well plates (1000 cells per well). The growth curve was determined by CCK8 assay according to the manufacturer (Sigma-Aldrich) instruction.

Colony formation assay and crystal violet staining

For colony formation assay, K30 and K450 cells were seeded into 12-well plates (1000 cells per well). The cells were then cultured under standard conditions for 10 days. After 10 days of culture, cells were fixed with 4% paraformaldehyde for 15 min at room temperature and then stained with 0.1% crystal violet for 5 min. After washing away excessive dye, cell colonies were visualized under a dissection microscope. Cell colonies consisting of more than 50 cells were counted and used for comparisons of colony formation ability.

Tumor sphere formation assay

For tumor sphere formation assay, cells were cultured in ultra-low attachment plates essentially as described [29]. In brief, cells were cultured in serum-free DMEM/F12 (Thermo Fisher Scientific, #11330-032) supplemented with 1% insulin (Thermo Fish Scientific, #17504044), 1% B27 (Thermo Fisher Scientific, #41400045), Pen/Strep (100 µg/ml; Thermo Fisher Scientific, #15140122), human recombinant epidermal growth factor (EGF; 20 ng/ml; R&B Systems, #236-EG-01M), and human recombinant basic fibroblast growth factor (bFGF; 10 ng/ml; R&B Systems, #233-FB-025/CF) in a humidified 5% CO_2 incubator at 37 °C. Fresh aliquots of EGF and bFGF were added and the serum-free media were changed every other day until the spheres formed. Spheres with a diameter over 40 µm were counted.

IHC staining and evaluation

Tissue microarray (TMA) construction and IHC staining were based on standard techniques as previously described [55]. Evaluating protein expression H score of IHC staining results of TMAs was as essentially described [56]. Briefly, we used Vectra 2.0.8 software for automated image acquisition and obtained the color images. Subsequently, the spectral libraries were constructed using Nuance 3.0 software. The color images were then evaluated by Inform 1.2 software following three steps: i) segmentation of the tumor region from the tissue compartments; ii) segmentation of the cells from the tumor region; and iii) calculation of the H score based on the optical density. The H score (=(% at 0) * 0 + (% at 1+) * 1 + (% at 2+) * 2 + (% at 3+) * 3) produces a continuous protein expression value in the range of 0 to 300[2].

Xenograft transplantation experiments

For xenograft transplantation, six-week-old nude mice (BALB/c nude) were purchased from Shanghai Jihui Laboratory Animal Care Company. The mice were maintained in an SPF animal facility of the East China Normal University and housed with standard 12 h light/dark cycles with food and water *ad libitum*. Animal experiments were carried out according to the *Guide for the Care and Use of Laboratory Animals* and approved by the Animal Ethics committee of China East Normal University. 1×10^6 parental K450 and K450 cells with stable overexpression of CHIP premixed with Matrigel Matrix (Corning, #354234) at a ratio of 1:1 were injected subcutaneously into the right and left flank regions, respectively. Tumor diameters from two perpendiculars (a: length; b: width) were measured by a vernier caliper and tumor volume (V, unit: cm^3) was calculated according to the equation: $V = a \times b^2 \times 0.52$.

Statistical analysis

All experiments were performed at least three independent times unless otherwise indicated. Statistical analysis and graphs were generated using GraphPad Prism 8.0 software. All statistical analyses were performed using an unpaired/paired two-sided t-test. The level of signification was set at $P < 0.05$, $P < 0.01$ and $P < 0.001$ for three independent experiments.

DATA AVAILABILITY

All data generated or analyzed during this study are included in this published article [and its supplementary information files].

REFERENCES

1. Avilion AA, Nicolis SK, Pevny LH, Perez L, Vivian N, Lovell-Badge R. Multipotent cell lineages in early mouse development depend on SOX2 function. Genes Dev. 2003;17:126–40.
2. Graham V, Khudyakov J, Ellis P, Pevny L. SOX2 functions to maintain neural progenitor identity. Neuron. 2003;39:749–65.
3. Sarkar A, Hochedlinger K. The sox family of transcription factors: versatile regulators of stem and progenitor cell fate. Cell Stem Cell. 2013;12:15–30.
4. Takahashi K, Yamanaka S. Induction of pluripotent stem cells from mouse embryonic and adult fibroblast cultures by defined factors. Cell. 2006;126:663–76.
5. Ferone G, Song JY, Sutherland KD, Bhaskaran R, Monkhorst K, Lambooij JP, et al. SOX2 is the determining oncogenic switch in promoting lung squamous cell carcinoma from different cells of origin. Cancer cell. 2016;30:519–32.
6. Mu P, Zhang Z, Benelli M, Karthaus WR, Hoover E, Chen CC, et al. SOX2 promotes lineage plasticity and antiandrogen resistance in TP53- and RB1-deficient prostate cancer. Science. 2017;355:84–8.
7. Novak D, Huser L, Elton JJ, Umansky V, Altevogt P, Utikal J. SOX2 in development and cancer biology. Semin Cancer Biol. 2020;67:74–82.
8. Porter L, McCaughan F. SOX2 and squamous cancers. Semin Cancer Biol. 2020;67:154–67.
9. Schaefer T, Lengerke C. SOX2 protein biochemistry in stemness, reprogramming, and cancer: the PI3K/AKT/SOX2 axis and beyond. Oncogene. 2020;39:278–92.
10. Tam WL, Ng HH. Sox2: masterminding the root of cancer. Cancer cell. 2014;26:3–5.
11. Weina K, Utikal J. SOX2 and cancer: current research and its implications in the clinic. Clin Transl Med. 2014;3:19.
12. Boumahdi S, Driessens G, Lapouge G, Rorive S, Nassar D, Le Mercier M, et al. SOX2 controls tumour initiation and cancer stem-cell functions in squamous-cell carcinoma. Nature. 2014;511:246–50.
13. Gangemi RM, Griffero F, Marubbi D, Perera M, Capra MC, Malatesta P, et al. SOX2 silencing in glioblastoma tumor-initiating cells causes stop of proliferation and loss of tumorigenicity. Stem cells. 2009;27:40–8.
14. Vanner RJ, Remke M, Gallo M, Selvadurai HJ, Coutinho F, Lee L, et al. Quiescent sox2(+) cells drive hierarchical growth and relapse in sonic hedgehog subgroup medulloblastoma. Cancer Cell. 2014;26:33–47.
15. Lim RZM, Mahendran HA, Malaysian Upper Gastrointestinal Surgical S. Esophageal squamous cell carcinoma and adenocarcinoma in Malaysia - Pooled data from upper gastrointestinal centers in a multiethnic Asian population. Cancer Epidemiol. 2022;80:102211.
16. Morgan E, Soerjomataram I, Rumgay H, Coleman HG, Thrift AP, Vignat J, et al. The global landscape of esophageal squamous cell carcinoma and esophageal adenocarcinoma incidence and mortality in 2020 and projections to 2040: new estimates from GLOBOCAN 2020. Gastroenterology. 2022;163:649–58.e642.
17. Sung H, Ferlay J, Siegel RL, Laversanne M, Soerjomataram I, Jemal A, et al. Global Cancer Statistics 2020: GLOBOCAN estimates of incidence and mortality worldwide for 36 cancers in 185 countries. CA Cancer J Clin. 2021;71:209–49.
18. Bass AJ, Watanabe H, Mermel CH, Yu S, Perner S, Verhaak RG, et al. SOX2 is an amplified lineage-survival oncogene in lung and esophageal squamous cell carcinomas. Nat Genet. 2009;41:1238–42.
19. Cancer Genome Atlas Research N, Analysis Working Group: Asan U, Agency BCC, Brigham, Women's H, Broad I. et al. Integrated genomic characterization of oesophageal carcinoma. Nature. 2017;541:169–75.

20. Cui Y, Chen H, Xi R, Cui H, Zhao Y, Xu E, et al. Whole-genome sequencing of 508 patients identifies key molecular features associated with poor prognosis in esophageal squamous cell carcinoma. Cell Res. 2020;30:902–13.
21. Maier S, Wilbertz T, Braun M, Scheble V, Reischl M, Mikut R, et al. SOX2 amplification is a common event in squamous cell carcinomas of different organ sites. Hum Pathol. 2011;42:1078–88.
22. Gen Y, Yasui K, Zen Y, Zen K, Dohi O, Endo M, et al. SOX2 identified as a target gene for the amplification at 3q26 that is frequently detected in esophageal squamous cell carcinoma. Cancer Genet Cytogenet. 2010;202:82–93.
23. Hussenet T, Dali S, Exinger J, Monga B, Jost B, Dembele D, et al. SOX2 is an oncogene activated by recurrent 3q26.3 amplifications in human lung squamous cell carcinomas. PloS One. 2010;5:e8960.
24. Alonso MM, Diez-Valle R, Manterola L, Rubio A, Liu D, Cortes-Santiago N, et al. Genetic and epigenetic modifications of Sox2 contribute to the invasive phenotype of malignant gliomas. PloS One. 2011;6:e26740.
25. Gen Y, Yasui K, Nishikawa T, Yoshikawa T. SOX2 promotes tumor growth of esophageal squamous cell carcinoma through the AKT/mammalian target of rapamycin complex 1 signaling pathway. Cancer Sci. 2013;104:810–6.
26. Cui CP, Zhang Y, Wang C, Yuan F, Li H, Yao Y, et al. Dynamic ubiquitylation of Sox2 regulates proteostasis and governs neural progenitor cell differentiation. Nat Commun. 2018;9:4648.
27. Fang L, Zhang L, Wei W, Jin X, Wang P, Tong Y, et al. A methylation-phosphorylation switch determines Sox2 stability and function in ESC maintenance or differentiation. Mol Cell. 2014;55:537–51.
28. Riggi N, Suva ML, De Vito C, Provero P, Stehle JC, Baumer K, et al. EWS-FLI-1 modulates miRNA145 and SOX2 expression to initiate mesenchymal stem cell reprogramming toward Ewing sarcoma cancer stem cells. Genes Dev. 2010;24:916–32.
29. Wang Z, Kang L, Zhang H, Huang Y, Fang L, Li M, et al. AKT drives SOX2 overexpression and cancer cell stemness in esophageal cancer by protecting SOX2 from UBR5-mediated degradation. Oncogene. 2019;38:5250–64.
30. Fang X, Huang Z, Zhai K, Huang Q, Tao W, Kim L, et al. Inhibiting DNA-PK induces glioma stem cell differentiation and sensitizes glioblastoma to radiation in mice. Sci Transl Med. 2021;13:eabc7275.
31. Edkins AL. CHIP: a co-chaperone for degradation by the proteasome. Subcell Biochem. 2015;78:219–42.
32. Pratt WB, Gestwicki JE, Osawa Y, Lieberman AP. Targeting Hsp90/Hsp70-based protein quality control for treatment of adult onset neurodegenerative diseases. Annu Rev Pharm Toxicol. 2015;55:353–71.
33. Seo J, Han SY, Seong D, Han HJ, Song J. Multifaceted C-terminus of HSP70-interacting protein regulates tumorigenesis via protein quality control. Arch Pharm Res. 2019;42:63–75.
34. Cox JL, Wilder PJ, Gilmore JM, Wuebben EL, Washburn MP, Rizzino A. The SOX2-interactome in brain cancer cells identifies the requirement of MSI2 and USP9X for the growth of brain tumor cells. PloS One. 2013;8:e62857.
35. Stankiewicz M, Nikolay R, Rybin V, Mayer MP. CHIP participates in protein triage decisions by preferentially ubiquitinating Hsp70-bound substrates. FEBS J. 2010;277:3353–67.
36. Su CH, Wang CY, Lan KH, Li CP, Chao Y, Lin HC, et al. Akt phosphorylation at Thr308 and Ser473 is required for CHIP-mediated ubiquitination of the kinase. Cell Signal. 2011;23:1824–30.
37. Hatakeyama S, Watanabe M, Fujii Y, Nakayama KI. Targeted destruction of c-Myc by an engineered ubiquitin ligase suppresses cell transformation and tumor formation. Cancer Res. 2005;65:7874–9.
38. Ding G, Chen P, Zhang H, Huang X, Zang Y, Li J, et al. Regulation of ubiquitin-like with plant homeodomain and RING Finger Domain 1 (UHRF1) protein stability by heat shock protein 90 chaperone machinery. J Biol Chem. 2016;291:20125–35.
39. Murphy ME. The HSP70 family and cancer. Carcinogenesis. 2013;34:1181–8.
40. Paul I, Ghosh MK. The E3 ligase CHIP: insights into its structure and regulation. Biomed Res Int. 2014;2014:918183.
41. Xu W, Marcu M, Yuan X, Mimnaugh E, Patterson C, Neckers L. Chaperone-dependent E3 ubiquitin ligase CHIP mediates a degradative pathway for c-ErbB2/Neu. Proc Natl Acad Sci USA. 2002;99:12847–52.
42. Matsumura Y, Sakai J, Skach WR. Endoplasmic reticulum protein quality control is determined by cooperative interactions between Hsp/c70 protein and the CHIP E3 ligase. J Biol Chem. 2013;288:31069–79.
43. Younger JM, Ren HY, Chen L, Fan CY, Fields A, Patterson C, et al. A foldable CFTRDeltaF508 biogenic intermediate accumulates upon inhibition of the Hsc70-CHIP E3 ubiquitin ligase. J Cell Biol. 2004;167:1075–85.
44. Banh A, Xiao N, Cao H, Chen CH, Kuo P, Krakow T, et al. A novel aldehyde dehydrogenase-3 activator leads to adult salivary stem cell enrichment in vivo. Clin Cancer Res. 2011;17:7265–72.
45. Ginestier C, Hur MH, Charafe-Jauffret E, Monville F, Dutcher J, Brown M, et al. ALDH1 is a marker of normal and malignant human mammary stem cells and a predictor of poor clinical outcome. Cell Stem Cell. 2007;1:555–67.
46. Li L, Wang L, You QD, Xu XL. Heat shock protein 90 inhibitors: an update on achievements, challenges, and future directions. J Med Chem. 2020;63:1798–822.
47. Metz EP, Rizzino A. Sox2 dosage: a critical determinant in the functions of Sox2 in both normal and tumor cells. J Cell Physiol. 2019;234:19298–306.
48. Mamun MMA, Khan MR, Zhu Y, Zhang Y, Zhou S, Xu R, et al. Stub1 maintains proteostasis of master transcription factors in embryonic stem cells. Cell Rep. 2022;39:110919.
49. Wang J, Zhang Y, Hou J, Qian X, Zhang H, Zhang Z, et al. Ube2s regulates Sox2 stability and mouse ES cell maintenance. Cell Death Differ. 2016;23:393–404.
50. Zhang C, Leng F, Saxena L, Hoang N, Yu J, Alejo S, et al. Proteolysis of methylated SOX2 protein is regulated by L3MBTL3 and CRL4(DCAF5) ubiquitin ligase. J Biol Chem. 2019;294:476–89.
51. Chen J, Ge X, Zhang W, Ding P, Du Y, Wang Q, et al. PI3K/AKT inhibition reverses R-CHOP resistance by destabilizing SOX2 in diffuse large B cell lymphoma. Theranostics. 2020;10:3151–63.
52. Kumar S, Basu M, Ghosh MK. Chaperone-assisted E3 ligase CHIP: a double agent in cancer. Genes Dis. 2022;9:1521–55.
53. Paul I, Ahmed SF, Bhowmik A, Deb S, Ghosh MK. The ubiquitin ligase CHIP regulates c-Myc stability and transcriptional activity. Oncogene. 2013;32:1284–95.
54. Yan S, Sun X, Xiang B, Cang H, Kang X, Chen Y, et al. Redox regulation of the stability of the SUMO protease SENP3 via interactions with CHIP and Hsp90. EMBO J. 2010;29:3773–86.
55. Xie JJ, Xu LY, Wu ZY, Zhao Q, Xu XE, Wu JY, et al. Prognostic implication of ezrin expression in esophageal squamous cell carcinoma. J Surg Oncol. 2011;104:538–43.
56. Huang W, Hennrick K, Drew S. A colorful future of quantitative pathology: validation of Vectra technology using chromogenic multiplexed immunohistochemistry and prostate tissue microarrays. Hum Pathol. 2013;44:29–38.

ACKNOWLEDGEMENTS

We thank all the other members of the JW laboratory for their suggestions and technical assistance. This study is supported by grants from the National Natural Science Foundation of China (32130051 to JW and 82002995 to ZW) and Science and Technology Commission of Shanghai Municipality (20JC1411500). It was also supported by the ECNU Public Platform for Innovation (011) and the Instruments Sharing Platform of the School of Life Sciences, East China Normal University.

AUTHOR CONTRIBUTIONS

LK, YW, and HZ were responsible for designing and conducting most of the experiments, extracting and analyzing data, and manuscript preparation. MC, JH, EL, and LX were responsible for tumor tissue microarray preparation, analysis, and data summary. PL, MX, and ZC conducted data validation. ZC and YH provided technical assistance. JL and RZ provided supervision and management. JW was responsible for supervision, funding, and manuscript preparation.

COMPETING INTERESTS

The authors declare no competing interests.

ADDITIONAL INFORMATION

Supplementary information The online version contains supplementary material available at https://doi.org/10.1038/s41388-023-02745-z.

Correspondence and requests for materials should be addressed to Rong Zhang or Jiemin Wong.